THERMAL PROPERTIES CHARACTERIZATION OF SPACE ELECTRONIC CIRCUITS VIA IMAGE-BASED VISUAL TECHNIQUES

Riccardo Monti[*], Paolo Gasbarri[†], Umberto Lecci[‡], and Marianna Lopatriello[§]

One of the main challenge of satellite manufacturers is its fully safety and complete operational functioning and, once a satellite is orbiting, the thermal management of its electronical equipment is one of the most significant issue. In order to verify if all the devices maintain high performances also under the thermal stresses point of view, it is always necessary to perform a detailed thermal analysis of the electronic equipment which of course requires that its thermal properties must be correctly identified. Usually thermal designers consider worst case conditions in order to simplify the numerical simulations and to ensure functionality and safety but when challenging operative condition, high power consumption are required, or more simply the dimension of the electronic devices are very small, the worst-case approach is not sufficient to take all the aspects of the thermal management under control. In this paper a general purpose in-house numerical code for the thermal characterization of printed circuit board will be proposed. This tool exploits the image-based visual reconnaissance technique to determine the exact distribution in terms of the conductive material mass fraction and in-plane mapping of very complex printed circuits in order to increase the descriptive level for high detailed thermal analyses. By considering the correct thermal conductivity of the circuits a more precise evaluation of the maximum temperatures reached during the operational life and in non-standard operative conditions could be handled reaching an improvement of the confidence with respect the overall equipment design.
Different study cases will be proposed and analyzed in the paper in order to underline the effective improvement of the thermal design coming from a more realistic characterization of the electronic devices.

INTRODUCTION

Printed circuit boards (PCB) are one of the most used technologies in the frame of electonic applications. Several subtechniques should be applied to achieve different results in terms of final electronic and thermal performances. Space technologies have particular attention to every detail in order to ensure high reliability and properly defined margin safety for the circuit and for the EEE components themselves.
The only way to achieve good performances with correct margin of safety is to enhance the thermal simulation numerical tool by considering more and more precise thermal characteristics in order to reduce the uncertainties coming from the analyses during the design process.
By looking at the thermal problem management one of the most significant issues is the correct estimation of the thermal conductivity of printed circuit to avoid temperature underestimation and/or

[*]Dr., ADHR GROUP - Agenzia per il Lavoro S.p.A., Via Collazia 8, 00183 Rome - IT.
[†]Prof., Mechanical and Aerospace Eng. Dept., University of Rome “Sapienza”, Via Eudossiana 18, 00135 Rome - IT.
[‡]Mr., Thermo-Mechanical Equipment Design Dept., Thales Alenia Space Italia, Via Saccomuro 24, 00131 Rome - IT.
[§]Ms., trasinee @ Thales Alenia Space Italia.

overestimation. In last decades many authors and many papers had been written about this topic and a lot of improvements are available to help the designers to do "the right choice"[1,2,3].
The main aim of this paper is to provide a dedicated tool in order to help the designers and the analylists in their daily job. In particular by exploiting a visual image automatic detetection the developed tool is able to estimate the quantities of copper, the conductor of PCBs, with respect to the insulator, typically polyamide and/or Thermount®.

PCB TECHNOLOGY DESCRIPTION AND THERMAL ANALYSIS METHODOLOGY

During the satellite on-orbit operating life the electronic equipment thermal management is one of the most significant issue.[4] As regards the on-board electronics, thermal problems which characterize such equipment are due to the *Joule effect*. In order to prevent damages and to ensure the proper functioning of all the on-board devices, during design phases a dedicated and detailed thermal analysis is mandatory. In order to perform an accurate thermal characterization of such equipment, the main aim of this study is the correct determination of thermal properties. In particular this paper is dedicated to the identification of the thermal characteristics of printed circuit boards.
A printed circuit board, commonly named PCB, mechanically supports and electrically connects electronic components using conductive tracks, pads and other features etched from copper sheets laminated onto an insulating substrate.[5] Two different techniques are used to set the various components onto a PCB: Trough Hole Technology (THT) and Surface Mount Technology (SMT). The first one is the classical technique which consists in the soldering of the electronic component leads onto a copper surface (pad) through the passage of these in holes made on the insulating support;[6] in the second one, particular devices named Surface Mount Devices (SMD) are used and the component is directly soldered onto the surface.[7] In order to reduce the sizing of the boards and to increase the integration level the PCB are layered constituting the so called *multi-layer circuit*.[8] A PCB for satellite applications is a multi-layer PCB: it is made up of several layers, some of them are metallized others not. The copper metallization thickness could be $70\ \mu m$, $35\ \mu m$ or $17\ \mu m$ while the typical PCB total thickness is about a few millimeters. Note that there are thermal vias which passes through the PCB thickness and interconnect the various layers.
In a multi-layer PCB the copper tracks are placed onto a composite insulating substrate usually made up of an epoxy matrix reinforced by glass and/or aramid fibers, such as the Thermount®.[9] Therefore, a PCB is a stratified structure made up of two materials which are very different from the thermo-mechanical point of view.[10] by taking this very complex architecture into account it is to understand that it is very arduous to identify the "real" thermal characteristics. In Table 1 some thermal and mechanical properties of copper and Thermount® are shown.

Table 1. Thermal and mechanical properties of materials commonly used for PCB

Material	$k\ [W/(m\ K)]$	$\alpha\ [ppm/K]$	$\rho\ [kg/m^3]$	$T^{melt}\ [K]$
Copper	391.00	9	8920	1357
Thermount®	0.70	17	1340	523

The thermal behavior characterization of a PCB is not simple and its importance is evident in order to ensure the PCB structural integrity and proper functioning. The identification of the real PCB thermal conductivity is crucial because this value must be used in the finite element model analysis suitable to verify also the compliance to the requirements prescribed by different space

programs specification and current ESA ECSS (European Space Agency-European Cooperation for Space Standardization) standards.[11]
In the complex industrial manifacturing process, the electronic equipment thermal design is taken under strict control by performing numerical analyses, e.g. finite element method (FEM) analyses, and experimental tests. Thermal boundary conditions are dictated by thermomechanical design constraints (for instance customer specifications) and define the maximum and minimum operating temperatures depending on the specific verification phase. Normally there are three verification phases: design phase, in which the temperature range is relative to the design operation; acceptance phase, in which the temperature range is obtained by adding/subtracting $5\ K$ to the design maximum/minimum temperatures; qualification phase, in which the temperature range is obtained by adding/subtracting $10\ K$ to the design maximum/minimum allowed temperatures. As far as thermal loads are concerned, they are derived from the Electric Design and consist in thermal power dissipation by the active components which are mounted onto PCB. Note that, as regards PCB finite element (FE) model, it is created by modeling only the printed board and not the relevant components mounted onto it. In fact, a complete FE model would be too complex to build up due to the presence of hundreds of electronic components mounted onto a real PCB.
In order to perform a thermal characterization as detailed as possible, the temperature of every component, which results from the FEM analysis, is increased by an amount which depends on its characteristics. In particular this value depends on the mounting technology. Electronics components may be soldered or glued and their thermal behavior will be different. In order to take this essential feature into account, it is possible to use the following formula:[11]

$$T^c = T^c_{FEM} + Q^c \cdot (R^{j-c} + R^{c-b}) \tag{1}$$

to represent the temperature of an active electronic component where in Eq. (1) Q^c is the power dissiption of the component measured in $[W]$, T^c_{FEM} is the temperature which results from the FEM analysis and corresponds to the position of the component with respect to the printed board and R^{j-c} and R^{c-b} respectively are the *junction-to-case* and the *case-to-board* thermal resistances which take into account the mounting characteristics and are measured in $[K/W]$.
The results of the analyses are evaluated by comparing them with the values prescribed by the current ESA ECSS standards which are the *derating* temperature,[11] in the design and acceptance phases, and the *rating* temperature,[11] in the qualification phase, for each electronic component. The rating and derating temperatures are prescribed by ESA ECSS standards and depend on the component type and on its manufacturing technology. A dedicated ESA ECSS standard is also relevant to the maximum temperature that the PCB reaches when power dissipation is applied. Other criteria are prescribed by company internal technological requirements. These rules are the thermal management guidelines.

NUMERICAL CODE

Code Architecture

Thermal properties of a PCB depend on the constituting materials, therefore, in order to simulate the real thermal behavior, the determination of the copper amount and its distribution are mandatory. For this purpose an in-house numerical code has been develope. It uses an image-based visual technique and it has been named ThAI TUL, acronym for Thermal Automatic Imaging Tool by University Lab.

ThAI TUL is a numerical code implemented in Matlab® environment and it operates by analyzing the black and white (B/W) images of every single metallized layer of the PCB. The images come from the electrical routing and they represent a map of the copper distribution (black) on Thermount® (white) in which the circuit tracks, the thermal vias traces and the components footprint.
The estimation process starts when the used imports all the layers images via ThAI TUL, the tool analyzes them, determines the effective copper amount, calculates the thermal conductivity and makes this information available to the user itself by providing a text output file and several figures. The ThAI TUL flowchart is shown in Figure 1. Every image imported in Matlab® is an RGB

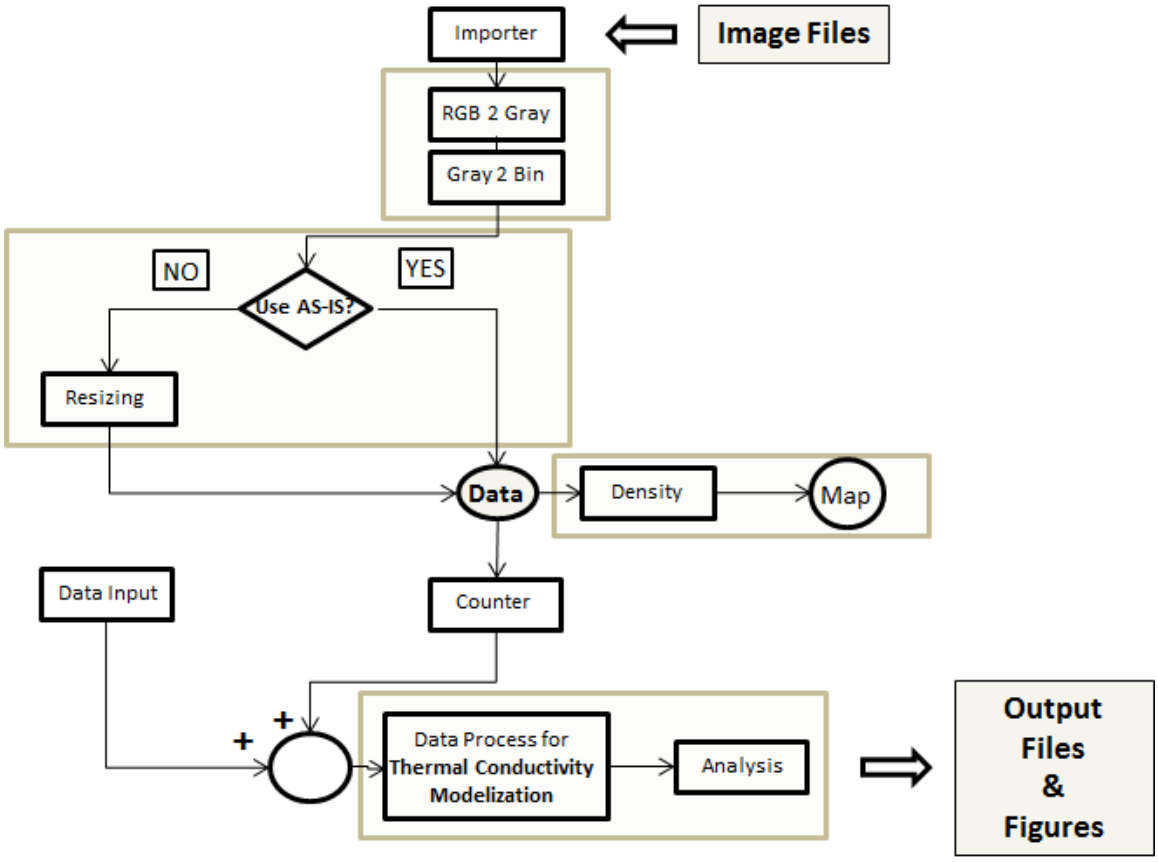

Figure 1. ThAI TUL flowchart

(Red-Green-Blue) image and it corresponds to a three-dimensional numerical array; the array size is m-by-n-by-3 where m and n are the number of pixels in the two directions, x and y respectively, in the image plane and each pixel is represented by a triplet of numbers. These numbers determine the intensity of red, green and blue which characterize the colored pixel. The code converts the RGB image in a binary B/W image and this means that the three-dimensional array is transformed in a two-dimensional m-by$n$ one, i.e. in a matrix composed just by 1 and 0: 1 represents the black pixel and 0 the white one. It is worth noting that, since the original images are B/W, this conversion does not involve loss of information and reduces the computational costs of the operations that will be made on the images. At this stage, the code determines the copper amount in the layer simply by counting the number of black pixels in the image.

By definining p^B and p^W the number of black and white pixels in the image respectively and with $p^{TOT} = m \cdot n$ the total number of pixels, then the fractions of copper ν^{Cu} and Thermount® ν^{Th} in the layer can be evaluated as follow: $\nu^{Cu} = p^B/p^{TOT}$ and $\nu^{Th} = p^W/p^{TOT}$.

Calculus of the Equivalent Thermal Conductivity

An equivalent value of the thermal conductivity could be evaluated through a *Rule of Mixtures*-like approach by using the volumetric fractions of copper ν^{Cu} and Thermount® ν^{Th} per each layer. This opportunity is given by the presence of the thermal vias which interconnect the different layers. Of course if there were no vias, this assumption would not be possible because of the insulating layers.
The thermal conductivity of the single layer i, which is characterized by the volumetric fractions ν_i^{Cu} and ν_i^{Th}, are given by:

$$k_i = \nu_i^{Cu} \cdot k^{Cu} + \nu_i^{Th} \cdot k^{Th} \tag{2}$$

where k^{Cu} and k^{Th} are the thermal conductivities of the copper and of the Thermount® respectively. Eq. (2) gives the in-plane thermal conductivity of the $i-th$ layer. The out-of-plane equivalent thermal conductivity k^{TOT} of the entire PCB could be obtained by taking the thermal conductivity of every $i-th$ layer into account, with $i = 1, ..., N_L$ and where N_L is the total number of metallized layers. It is worth underlining that t^{TOT} is the PCB total thickness, t^{Cu} is the copper metallization thickness and $t^{Th} = t^{TOT} - \sum_{i=1}^{N_L} t_i^{Cu}$ is the total Thermount® thickness. On account of this we can define the copper and Thermount® thickness fractions as $h^{Cu} = t^{Cu}/t^{TOT}$ and $h^{Th} = t^{Th}/t^{TOT}$ respectively. The equivalent out-of-plane thermal conductivity of the entire PCB can finally be written as:

$$k^{TOT} = h^{Th} \cdot k^{Th} + \sum_{i=1}^{N_L} h^{Cu} \cdot (\nu_i^{Cu} \cdot k^{Cu} + \nu_i^{Th} \cdot k^{Th}) \tag{3}$$

Eq. (3) will give the real PCB thermal behavior for the heat conduction analysis. In fact it takes both the real copper percentage in every metallized layer and its distribution along the thickness into account.

Mapping of the Copper Density

In order to have more detailed information about the out-of-plane thermal conductivity, ThAI TUL offers the opportunity to obtain a copper distribution mapping for each layer. This mapping could be obtained with the desired accuracy by choosing the discretization size as explained in the following.
After the image processing, the numerical tool provides the number of rows r and columns c of the binary matrix **A** in which the number of black and white pixels is contained. The number of all pixels is $r \times c$. The user of ThAI TUL can select the number of elements needed for the discretization by directly introducing the numbers p of divisions in x direction and q in y direction in the image plane. In this way, the user chooses the number $p \times q$ of padding matrices in which the binary matrix will be discretized. Through this information, the numerical code calculates the copper density by counting the number of black pixels in each pad and then by dividing this value by the number of all pixels in the pad itself.
The pad matrix size is m-by-n where m and n are the nearest integer less than or equal to r/p and c/q respectively. It is worth noting that since r and c might not be integer multiples of p and q, some rows and columns could be excluded and consequently the choice of p and q is crucial in order to

have no loss of information.
Therefore, the binary matrix **A** is discretized in $p \times q$ pads which have indices k, l, with $k = 1, .., p$ and $l = 1, ..., q$. Every pad is a binary matrix and the relevant number of black pixels could be obtained by summing all the pad elements/coefficients. By repeating this operation for each pad, and then by dividing this value by $m \cdot n$, a value ρ_{kl} of copper density may be associated to each pad as follows:

$$\rho_{kl} = \sum_{i=1}^{m} \sum_{j=1}^{n} \frac{a_{ij}^{kl}}{m \cdot n} \tag{4}$$

where a_{ij}^{kl} is the element corrisponding to $i-th$ row and $j-th$ column in the pad which has indices kl.

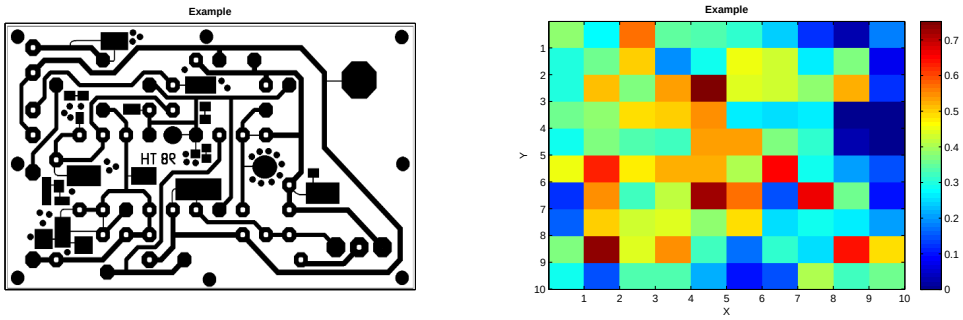

(a) Example of B/W image (b) Copper distribution discretization ($p = q = 10$)

Figure 2. Example of ThAI TUL Analysis

In this way, a new p-by-q matrix **D** with components ρ_{kl} is obtained. **D** is the copper density matrix. By observing Eq. (4), we may immediately deduce that $\rho_{kl} \in [0, 1]$.
In Figure 2 an example of a B/W layer image and its relative copper distribution discretization are shown; in this case the values $p = 10$ and $q = 10$ have been chosen. A very simple proof of the

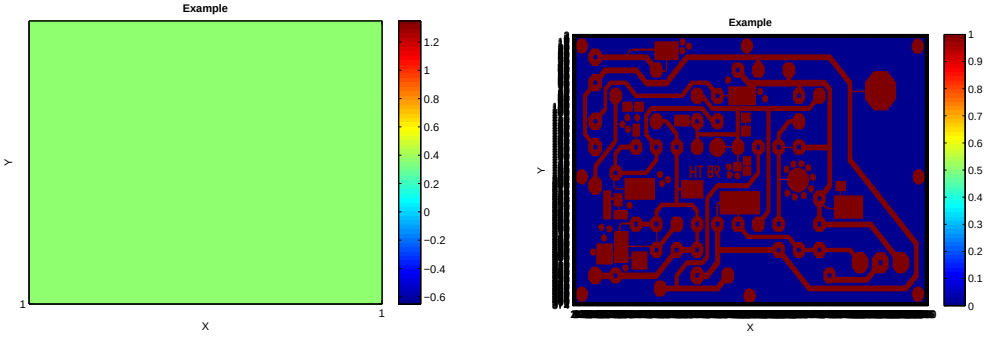

(a) Maximum size pad matrix ($p = q = 1$) (b) Minimum size pad matrix ($p = r,\ q = c$)

Figure 3. Different choice for discretization

tool well-functioning can be achieved if the user selects $p = r$ and $q = c$, i.e. the minimum pad size, then **D**=**A** and ThAI TUL reconstructs the initial image of the layer by mapping the copper

density. On the other end, if the user selects $p = q = 1$, i.e. the maximum pad size, the matrix $\mathbf{D}$ is transformed in a unique scalar value which is the average copper density value for the entire layer. Figure 3 shows the two copper distribution maps above estimated.

Split of the Printed Circuit Board into Macro-Partitions

ThAI TUL allows to the user to import any number of images and analyzes it simultaneously, in order to have information about the real behaviour of the entire printed circuit board. It provides the copper percentage and the insulator percentage in every metallized layer and in the whole PCB, the copper density map for each layer and a thermal conductivity equivalent value for the entire printed circuit board. The designer usually uses a single average thermal conductivity value for the PCB in the numerical thermal analysis but, because of the particular copper distribution, he may want to obtain different thermal conductivity values for some regions into which he discretizes the printed board. If the designer selects the option of ThAI TUL which uses the same number of pads for all the metallized layers, the numerical code provides an average copper density mapping in the entire PCB in order to allow the user to assess how many macro-partitions are necessary to characterize the PCB thermal behaviour. So, if N_L is the number of metallized layers, N_L matrices $\mathbf{D_s}$ are obtained, where $s = 1, ..., N_L$, and all the matrices have the same size p-by-q. In this way, the average copper density matrix $\tilde{\mathbf{D}}$ could be obtained by summing up all the matrices $\mathbf{D_s}$ and then by dividing this sum by the number of layers N_L:

$$\tilde{\mathbf{D}} = \sum_{s=1}^{N_L} \frac{\mathbf{D_s}}{N_L} \tag{5}$$

The average density permits to the designer to know the real copper distribution in the PCB, not only along the thickness in the printed board, but also in the plane. The heat diffusion depends on the copper amount and on its distribution, therefore, there could be areas of the PCB in which the out-of-plane thermal conductivity is higher, because of the greater copper amount, and areas in which it is appreciably lower. The average copper density map allows the designer to decide if he needs different thermal conductivity values and how many partitions are necessary.
At this stage, after observing the average copper density mapping, the designer selects the number of macro-partitions in which he would split the printed board by inserting the sub-divisions number p_R in x direction and the sub-divisions number q_R along the y direction. In this way, the PCB is divided in $M_R = p_R \times q_R$ macro-partitions.
In the case of macro-partitions, ThAI TUL determines the copper density by means the same algorithm used for each metallized layer but directly on the matrix $\tilde{\mathbf{D}}$. By exploiting this kind of approacg the copper density and the consequent value of each macro-partition thermal conductivity is the average value of the average value. The M_R copper density values are ν_l^R, where $l = 1, ..., M_R$, so the thermal conductivity of each macro-reagion k_l^R may be obtained as follows:

$$k_l^R = h^{Th} \cdot k^{Th} + N_L \cdot h^{Cu} \cdot (k^{Cu} \cdot \nu_l^R + k^{Th} \cdot (1 - \nu_l^R)) \tag{6}$$

Eq. (6) is a further average operation and as a conseguence of the fact in the numerical thermal analysis we will suppose that each layer has the same copper average distribution.
In Figure 4 the average copper density and an example of split into macro-areas of a PCB analyzed via ThAI TUL are shown. Furthermore, in Table 2 the corresponding thermal conductivity values calculated by ThAI TUL and the percentage difference between the singular macro-partition value

and the average one have been reported. It is worth noting that these values are appreciably different.

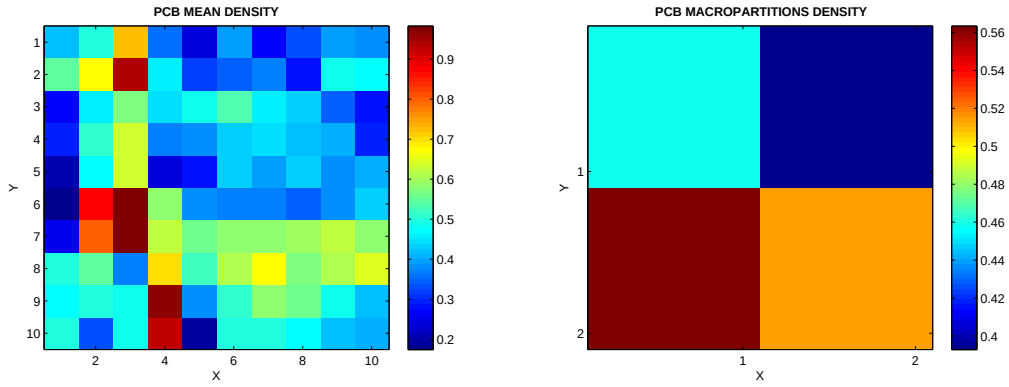

(a) Average copper density in a PCB

(b) Split into macro-partitions

Figure 4. Example of application on a real multi-layer PCB

Table 2. Thermal conductivity of macro-partitions and entire PCB in Figure 4

Macro-partition	1-1	1-2	2-1	2-2	TOT
$k\ [W/(m\ K)]$	28.52	34.91	24.55	31.87	29.86
$\Delta k = 100\dfrac{k^R - k^{TOT}}{k^{TOT}}\ [\%]$	-4.49	16.91	-17.78	6.73	–

Code Validation

Each developed numerical code needs to be validated in order to be confident with the obtained results. The most suitable manner to validate a in-house or a commercial code is to compare the obtained results with an analytical solutions if any. The difference among solution gives us a feeling about the quality of the developed software.
The most significative code validation is the comparison of the calculated fractions with respect to the fractions obtained via an uncorrelated method.
The validation method is based on classic matrices algebra. Let us to consider a rectangular matrix m-by-n and consider the general concept of matrix norm defined as follows:[12]

$$\left\|\mathbf{A}\right\|_p = \left(\sum_{i=1}^{m}\sum_{j=1}^{n}\left|a_{ij}\right|^p\right)^{\frac{1}{p}} \tag{7}$$

where if the index p is equal to 2 the *Frobenius norm* is obtained and it will read as follows:

$$\left\|\mathbf{A}\right\|_2 = \left\|\mathbf{A}\right\|_F = \sqrt{\theta(A\cdot A^T)} = \sqrt{\sum_{i=1}^{\min(m,n)}\lambda_i^2} \tag{8}$$

where $\theta(\mathbf{A}\cdot\mathbf{A}^T)$ is the trace of the matrix $\mathbf{A}$ and λ_i is the $i-th$ singular value of the matrix $\mathbf{A}$. By expressing the trace for each component of the matrix we have that $\theta(\mathbf{A}\cdot\mathbf{A}^T) = \sum_{i=1}^{m}\sum_{j=1}^{n} a_{ij}\cdot$

a_{ji}.
Let now suppose that the matrix $\mathbf{A}$ is a binary matrix, corresponding to a B/W image, where each generic element a_{ij} can assume values equal to 1 or to 0. By taking the type of the coefficients into account the trace is simplified and we have $\theta(\mathbf{A}\cdot\mathbf{A}^T)=\sum_{i=1}^{m}\sum_{j=1}^{n}a_{ij}$ and for analogy the singular value will be defined as:

$$\sqrt{\sum_{i=1}^{m}\sum_{j=1}^{n}a_{ij}}=\lambda_i \tag{9}$$

where $i=1,\ldots,n$ and in particular for $i>1$ $\lambda_i=0$ by definition of binary matrix.
Since the calculation of the singular value corresponds to the sum of the matrix coefficients that for binary matrix is equal to the black pixels number Eq. (9) is the relation needed to validate the developed numerical code. In order to evaluate the singular value of the matrix $\mathbf{A}$ a classical *Single Value Decomposition* technique is here adopted which reads as follows:

$$svd(\mathbf{A})=\mathbf{L}\ \ \mathbf{\Lambda}\ \ \mathbf{R} \tag{10}$$

where the matrix $\mathbf{L}$ is a m-by-m matrix cointaining the left eigenvectors, $\mathbf{\Lambda}$ is a m-by-n matrix cointaining the eigenvalues and eventually $\mathbf{R}$ is a n-by-n matrix containing the right eigenvectors.[12]
The matrix $\mathbf{\Lambda}$ has the following structure:

$$\mathbf{\Lambda}=\begin{pmatrix}\lambda_1 & \mathbf{0}\\ \mathbf{0} & \mathbf{0}\end{pmatrix} \tag{11}$$

on account of this it is possible to construct a second matrix $\tilde{\mathbf{A}}$ by employing the obtained eigenvectors and a new matrix of eigenvalues $\tilde{\mathbf{\Lambda}}$ where the only not-null term is calculated from Eq. (9):

$$\tilde{\mathbf{\Lambda}}=\begin{pmatrix}\sqrt{\theta(\mathbf{A}\cdot\mathbf{A}^T)} & \mathbf{0}\\ \mathbf{0} & \mathbf{0}\end{pmatrix} \tag{12}$$

By exploiting a second singular value decomposition is possible to derive also the new set of eigenvalue and eigenvectors, and in particular we have:

$$svd(\tilde{\mathbf{A}})=\overline{\mathbf{L}}\ \ \overline{\mathbf{\Lambda}}\ \ \overline{\mathbf{R}} \tag{13}$$

Note that $\overline{\mathbf{\Lambda}}=\tilde{\mathbf{\Lambda}}$ is always valid for the eigenvalues matrix. To complete the validation of the numerical code it is necessary a last step. In fact the eigenvectors extracted by the matrix $\mathbf{A}$ must be compared with those extracted by the new matrix $\tilde{\mathbf{A}}$. An efficient tool for this comparison can be found in the MAC (*Modal Assurance Criterion*)[13] normally used to verify the auto and cross-correlation between numerically calculated and experimentally determined modal shapes.[14] The $\mathbf{MAC}$ parameter is defined as follows:

$$\mathbf{MAC}=\left[(\mathbf{\Psi}_n^T\mathbf{\Psi}_n)\cdot(\mathbf{\Psi}_e^T\mathbf{\Psi}_e)\right]^{-1}\cdot\left(\mathbf{\Psi}_n^T\cdot\mathbf{\Psi}_e\right)^2 \tag{14}$$

where $\mathbf{\Psi}_n$ is the rectangular matrix containing the numerically computed eigenvectors and $\mathbf{\Psi}_e$ is the rectangular matrix containing the experimentally identified modal shapes. If the two sets of eigenvectors are fully correlated the MAC is a diagonal unitary matrix, viceversa the uncorrelated modes are null.[15]
In the case of the in-house developed numerical code the experimental matrix is associated to the

initial eigenvectors set with $\mathbf{\Psi}_e = \mathbf{L}$ or $\mathbf{\Psi}_e = \mathbf{R}$ and the numerical matrix is associated to the other set $\mathbf{\Psi}_n = \overline{\mathbf{L}}$ or $\mathbf{\Psi}_n = \overline{\mathbf{R}}$. The criterion shall be applied to both eigenvector set in order to fully validate the proposed methodology. If the calculated $\mathbf{MAC}_L$ and $\mathbf{MAC}_R$ are unitary matrices the validation is completed and considere succeffully.
In order to verify the effective validation of the numerical code we considered a generic 10-by-15 rectangular matrix entirely null with the exception of a non-symmentric inner unitary area. This area is a 4-by-4 area, see Figure 5. By considering the previous relation it is possible to evaluate the

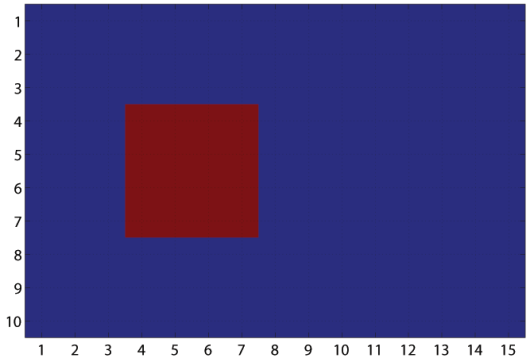

Figure 5. Auto & Cross-correlation

norm of the matrix such as the sum of elements that leads to $\lambda_1 = 16$ and the relevant singular value that in this case is equal to $\sigma_1 = +\sqrt{\lambda_1} = 4$. By using a classical commercial and numerical tools (in this case Matlab®) it was possible to evaluate the *Single Value Decomposition* of the original matrix and of the matrix built up by using the eigenvalue calculated via ThAI TUL. In addition to this the MAC_L and MAC_R were evaluated and hereafter represented in Figure 6.

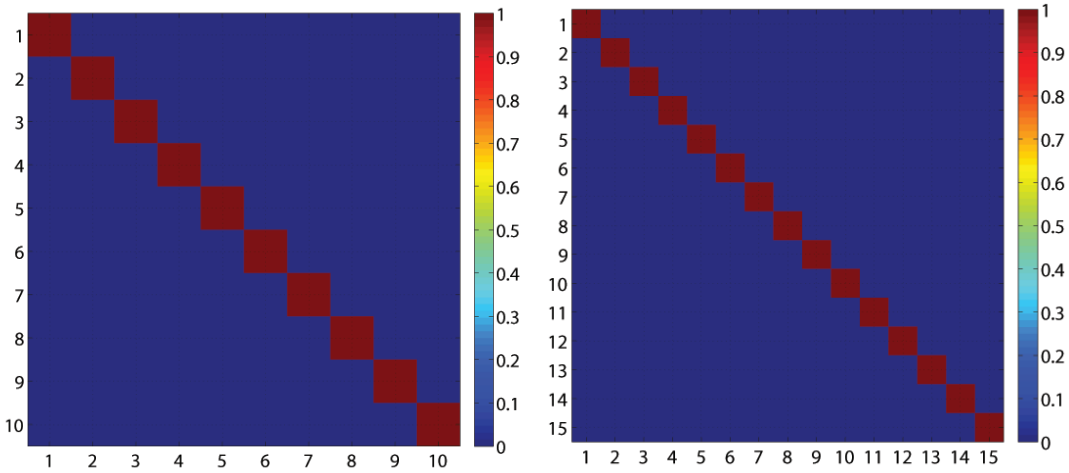

(a) $\mathbf{MAC}_L$ fot left eigenvectors (b) $\mathbf{MAC}_R$ fot right eigenvector

Figure 6. Auto & Cross-correlation

By the above results it was possible to state that ThAI TUL is able to correctly evaluate the presence of black pixels and this step determine the possibility to properly compute the volumetric

fraction of copper and insulator relevant to each layer of the PCB under consideration.

NUMERICAL SIMULATIONS

The improvments on thermal analyses derived by the use of ThAI TUL will be demonstrated through several numerical simulations. In the following some results of the FEM analyses are shown.

At present, the analysts determine the thermal conductivity of the PCBs by observing the plot of the PCBs metallized layers and by evaluating the copper percentage in the printed circuit board. They use the semi-empirical formula $k = 8.42 \cdot N$, where N represents the number of *thermal layers*. Please note that in general $N \neq N_L$.As per generic assumptions layer is considered as a thermal layer when its copper percentage is estimated greater than 60%. The identification of thermal conductivity is based only on the subjective evaluation of the designer and/or of the analyst. The use of ThAI TUL allows to overcome the uncertainty associated to this empyrical approach increasing the confidence with the numerical simulation results.

The numerical results presented in this section are obtained by analyzing the PCB shown in Figure 4. It is a multi-layer PCB for space equipment application made up of 8 layers and its copper distribution allows the designers to consider from 2 to 4 thermal layers. In Table 3 it is possible to read and compare the thermal conductivity values obtained in the cases of $N = 2$ (worst case) and $N = 4$ with respect to the value provided by ThAI TUL.

Table 3. Evaluations of the thermal conductivity of the PCB shown in Figure 4

Case	$k^{N=2}$	$k^{N=4}$	$k^{ThAITUL}$
$k\ [W/(m\ K)]$	16.42	33.68	29.86

By considering $N = 2$, in accordance with the worst case philosophy,[16] thermal conductivity is lower than the value provided by ThAI TUL, while, by considering $N = 4$, it is too much higher. We have to observe that a thermal conductivity higher than the real one is dangerous because it could hides the zones of the circuit where the heat diffusion might result critical; of course this situation must be avoided. Nevertheless a value of thermal conductivity lower than the real one must also be avoided. In the latter case this could represents a worst case that could add a high margin of safety to the design, which in turn produces a not thermally optimized PCB final product.

In order to provide a demonstration of the improvements brought by ThAI TUL two different FEM thermal analyses relevant to the PCB reported in Figure 4 have been performed. The forst one was performed by considering the thermal conductivity value relative to $N = 2$ thermal layers and the other one by considering the results achieved via ThAI TUL.

Several electronic components are mounted onto this PCB. The applied electrical feed generates different values of power dissipation. The thermal load is in the range of $Q = 20\ mW$ up to $Q = 1250\ mW$. Furthermore, they have different values of R^{j-c} and R^{c-b} (see Eq. (1)) due to different mounting technique. The Thermal analyses are performed by imposing a uniform thermal boundary condition, which value depends on the verification design phase. All the components have the same derating temperature $T^{der} = 110\ ^\circ C$ and the same value of rating temperature $T^r = 150\ ^\circ C$ whereas the maximum allowed temperature for the printed board is $85\ ^\circ C$.

In Table 4 some thermal analysis results obtained by adopting the value $k^{N=2}$ (see Table 3) are reported. Note that the simulation is relative to the acceptance design phase, therefore, each elec-

tronic component's temperature T must not exceed its T^{der}; the boundary condition temperature is $T_0 = 65\ ^\circ C$. Note also that in Table 4 the thermal resistance value $R = R^{j-c} + R^{c-b}$ is shown for each component. The abbreviations appearing in the table (normally called reference designator) have the following meanings: CR indicates a diode, Q a transistor, T a transformer and eventually U is an integrated circuit.

Table 4. FEM thermal analysis results in the acceptance phase obtained by adopting the thermal conductivity corresponding to $N = 2$

Component	CR5	Q1	Q4	T2	U3
$R\,[K/W]$	1.9	1.7	5.1	1.3	75.4
$T^{FEM}\ [^\circ C]$	83.3	92.1	92.1	86.9	81.6
$T\ [^\circ C]$	84.1	93.9	98.5	88.0	111.8
$T^{der}\ [^\circ C]$	110.0	110.0	110.0	110.0	110.0

By observing the values in Table 4, we can deduce that for components Q1, Q4 and T2, the relevant temperature T^{FEM} overcomes the threshold value set for the PCB; moreover, in the case of the component U3 the temperature T results to be not compliant with the requirement imposed by ESA ECSS standards because its value results higher than T^{der}. It is worth observing that this value of temperature is due to the high thermal resistance of the component U3. We can conclude that under these conditions the printed circuit board is not compliant with the ESA requirements and that the design must be modified.
In Table 5 the thermal analysis results obtained by using the corrected values provided by ThAI TUL are reported. The Thermal conductivity values employed for this analysis have been obtained by splitting the PCB into four macro-regions and the relevant values are reported in Table 2.

Table 5. FEM thermal analysis results in the acceptance phase obtained by adopting the thermal conductivity provided by ThAI TUL

Component	CR5	Q1	Q4	T2	U3
$T^{FEM}\ [^\circ C]$	74.4	78.6	78.6	76.1	75.2
$T\ [^\circ C]$	75.1	80.4	84.9	77.2	105.2
$T^{der}\ [^\circ C]$	110.0	110.0	110.0	110.0	110.0

As one could expect, by looking at Table 5, the thermal analysis provides result completely different from the previous one. And the PCB board results demonstrate full compliance to the ESA ECSS standards requirement.
This result has a strong validity both from the technical point of view and from the industrial one because it demonstrates that by increasing the confidence of the designers with respect to the thermal charactetization the reliability of the numerical analyses is increased and it can provide a considerable saving of resources by avoiding unuseful stops in the design process.

CONCLUSION

This article has highlighted the opportunity to increase the confidence of the designer with the PCBs thermal characterizaiton in order to have a correct thermal management by using a numerical tool based on a visual technique. The foregoing arguments show that the use of a code such as ThAI

TUL help the designers to obtain reliable and detailed information in an immediate and simple way to identify the PCBs thermal behavior as well as better. Furthermore, ThAI TUL provides a number of advantages: it is simple to use because it has an appropriate interface which to guide the user; it is portable because it can be used on any computer where Matlab® is installed in and it can be interfaced with FEM softwares, like commercial MSC.Nastran. The latter one offers a very wide range of application such as the thermo-mechanical optimization that allows to increase the importance of the identified pros.

By using an appropriate numerical strategy which combines the use of optimization algorithms and FEM analysis, the lowest thermal conductivity values for the entire PCB and for every macro-partition in which it was split can be determined in order to be compliant with the thermal requirements. The authors have found in this aspect the object of future activity where the detailed characterization will be used as a key stone of a more complex optimization activity.

ACKNOWLEDGMENT

A sincere and a grateful thanks to all the colleagues of the Thermo-mechanical Equipment Design Department of Thales Alenia Space Italia and in a special manner to Mr. Fabio Felici to help us in brainstorming and numerical tool debug.

REFERENCES

[1] F. Sarvar, "PCB glass-fibre laminates: Thermal conductivity measurements and their effect on simulation," *Journal of Electronic Materials*, Vol. 19, Issue 12, 1990.

[2] Y. Shabany, "Component size and effective thermal conductivity of printed circuit boards," *Proceeding of Thermal and Thermomechanical Phenomena in Electronic Systems*, 2002, 10.1109/ITHERM.2002.1012496.

[3] T. F. Lemczyk, "PCB Trace Thermal Analysis and Effective Conductivity," *Journal of Electronic Packaging*, 1992, 10.1115/1.2905474.

[4] A. Maini and V. Agrawal, *Satellite Technology - Principles and Applications*. John Wiley & Sons Ltd. Publications, second ed., 2011. ISBN 978-0-470-66024-9, India.

[5] C. T.Robertson, *Printed Circuit Board-Designer's Reference: Basic*. Prentice Hall PTR, 2004. ISBN 0130674818, NJ, USA.

[6] R. Prasad, *Surface Mount Technology Principles and Practices*, Vol. 1. Springer US, 1988. ISBN 0442205279, New York, USA.

[7] J. Varteresian, *Fabricating Printed Circuit Boards*. Butterworth-Heinemann, 2002, UK.

[8] C. Harper, *High Performance Printed Circuit Boards*. McGraw-Hill Education, 2000, USA.

[9] A. VV, *Electronics Material Handbook-Packaging*, Vol. 1. ASM International, 1989, USA.

[10] M. Jawitz, *Printed Circuit Board Materials Handbook*. McGraw-Hill Education, 2005, USA.

[11] ESA Requirements and Standards Division, *Space product assurance-Derating-EEE components*, 2010. ECSS-Q-ST-30-11C Rev.1, Noordwijk, NL.

[12] L. N. Threfeten and D. B. III, *Numerical Linear Algebra*. Society for Industrial and Applied Mathematics, third ed., 1997, Philadelphia, USA.

[13] D. Ewins, *Modal Testing: Theory, Practice and Application*. John Wiley & Sons Ltd. Publications, second ed., 2000. ISBN 9780863802188, USA.

[14] M. P. e. al., "Modal Assurance Criterion," *Procedia Engineering*, Vol. 48, 2012. Elsevier Ltd.

[15] M. Rades, *Mechanical Vibrations II Structural Dynamic Modelling*. Editura PRINTECH, 2010.

[16] ESA Requirements and Standards Division, *Space product assurance-Worst case analysis*, 2011. ECSS-Q-HB-30-01A, Noordwijk, NL.